

2-23-2014

Laboratory Study of the Effect of Electromagnetic Waves on Airflow during Air Sparging

Atena Najafi

Boise State University

Vahab Bolvardi

Boise State University

Arvin Farid

Boise State University

Jim Browning

Boise State University

Elisa Barney Smith

Boise State University

Laboratory Study of Effect of Electromagnetic Waves on Airflow during Air Sparging

Atena Najafi

Graduate Research Assistant
Department of Civil and Environmental Engineering
Boise State University

Vahab Bolvardi

Graduate Research Assistant
Department of Civil and Environmental Engineering
Boise State University

Arvin Farid

Associate Professor
Department of Civil and Environmental Engineering
Boise State University

Jim Browning

Associate Professor
Department of Electrical and Computational
Engineering
Boise State University

Elisa Barney Smith

Associate Professor
Department of Electrical and Computational
Engineering
Boise State University

Abstract

Air sparging is a technique that uses the injection of a gas (e.g., air, oxygen) into the subsurface to remediate saturated soils and groundwater contaminated with volatile organic compounds (VOCs). During air sparging, air or oxygen is injected into the subsurface below the lowest known depth of chemical contamination. The injected air will rise through the contaminated zones by buoyancy. Contaminant removal efficiency and air sparging performance are highly dependent on the pattern and type of airflow. Airflow, however, suffers from air channel formation (i.e., preferential paths for airflow), limiting remediation to smaller contaminated zones. This paper presents the results of experimental work investigating the possibility of controlling and improving airflow patterns through a saturated glass-bead medium using electromagnetic (EM) waves to enhance air sparging. The test setup consists of a resonant cavity made of an acrylic tank covered with transparent, electrically conductive films. Experimental measurement of the electric field component of EM waves is performed at different frequencies. Airflow pattern is also studied at different air-injection pressure levels with/without EM stimulation. The zone of influence (ZOI) during air sparging is monitored using digital imaging. A quantitative approach is then taken to correlate the characteristics of EM waves and airflow patterns.

Keywords: Airflow, Air-Channel Formation, Electromagnetic Wave, Zone of Influence.

1. INTRODUCTION

Groundwater contamination is a crucial concern to most federal and state agencies. This concern is especially significant given that about 23% of the freshwater used in the United States in 2005 came from groundwater sources (U.S.G.S., 2005). Chemical and gasoline spills or leaking underground storage tanks are sources of groundwater contamination. Accidental spills and improper disposal practices have also led to groundwater degradation. Environmentally hazardous spills of chemicals and gasoline are very important when directly contaminating ground water. Groundwater contamination with these petroleum products has become a widespread problem and created the need for urgent attention by various federal and state agencies. All chemical spills, potentially affecting groundwater, need to be remediated quickly and efficiently.

Air sparging is an in-situ technique used for remediation of groundwater and saturated soils contaminated with volatile organic compounds (VOCs). Air sparging came into existence about 1985 in Germany and is becoming increasingly more popular in the United States. Air sparging is, however, limited by random air-channel formation (Elder and Benson, 1999), which creates a limited mass transfer zone (MTZ) within and adjacent to formed air channels (Braida and Ong,

2001). Therefore, the current air sparging practice can take months or years, rendering it costly and ineffective, leading to incomplete remediation. One of the most popular methods to enhance air sparging's effectiveness is pulsating the air sparging pumps (Benner et al., 2002).

Another method used to enhance several remediation technologies, potentially applicable to air sparging, is the use of direct electric current (DC) or alternating electric current (AC) in saturated soils (Suthersan, 1999). The use of DC and AC can potentially help enhance air sparging. When DC is used, contaminant transport and the flow of oxygen can be generated or controlled in the direction of the electric current. Although the heat produced by DC or AC enhances the diffusion between air channels, there may be adverse effects on microbial activities within soil due to the uncontrolled and high amount of generated heat. However, the possibility of reducing the generated heat and/or negative environmental impacts due to overheating of organisms were not investigated enough. The riving effect of the EM waves was not studied either. This study focuses on the major goal of using electromagnetic waves to enhance air sparging while the generated heat is minimized. The first step of this study was developed and conducted by Azad et al. (2013) to determine the effects of EM stimulation on diffusion of a nonreactive dye in water as a visible analogy to air sparging. In this work, the same effect is studied directly on airflow within porous media. This paper presents the result of a laboratory study investigating airflow patterns in water-saturated zones under air sparging conditions with and without applying EM waves.

2. Background

2.1. EM-Wave Propagation

The major task of this study is to correlate various transport mechanisms controlling airflow to the electric-field component of EM waves launched into porous media. The relations between the fundamental electromagnetic quantities are governed by Maxwell's equations. Maxwell's' equation are a set of equations written in either differential or integral form (Balanis, 1989). The differential form is as follows.

$$\nabla \times \vec{H} = \vec{J} + \frac{\partial \vec{D}}{\partial t} \quad (1)$$

$$\nabla \times \vec{E} = -\frac{\partial \vec{B}}{\partial t} \quad (2)$$

2.2. Airflow through Advection, Dispersion, and Diffusion

Advection is the transfer of a phase by the flow of the background fluid. The flow rate (flux) of both groundwater and soil gas is governed by Darcy's Law. The rate of transport of the background water is a function of permeability, which in turn depends on the grain-size distribution, the type and structure of the soil, the porosity, and the water-content of the soil as well as the viscosity and density of the permeant fluid (Semer and Robin, 1998).

Dispersion is the spreading or dilution of a substance (e.g., contaminants) within a background (e.g., groundwater or soil gas) through mixing or molecular diffusion. Pulsating of air-sparging pumps aids air sparging through a dispersion process. Pulsation of air-sparging pumps also helps air sparging through creating potential new channels in zones of soil where air channels were not formed in the previous cycles of pulsation (Semer and Robin, 1998).

Diffusion is the process where the diffusing matter (e.g., contaminant) moves from an area of high concentration to an area of low concentration in order to reduce the concentration gradient until the concentration gradient diminishes. Diffusion is hence governed by the second Fick's law.

$$\frac{\partial C}{\partial t} = -\vec{\nabla} \cdot (\vec{F}) \quad (3)$$

where C is the concentration of the diffusing matter (g/m^3); and $\vec{F} = -\vec{D}\vec{\nabla}C$ = the diffusion flux ($\text{g}/\text{m}^2\text{s}$) of the diffusing matter, which, according to the first Fick's law, is proportional to the gradient of the concentration of the substance (.....,), where \vec{D} is the diffusion coefficient tensor (m^2/s).

2.3. Major Design Factors for Air Sparging Systems

A working knowledge of the extent and nature of airflow through saturated soils is important in order to find the optimum design of technologies to enhance air sparging and the estimation of the field performance. The zone of influence (ZOI) is defined as the region of soil treated by a given injection or extraction well. The radial distance from the well to the outer edge of the zone of influence is known as the radius of influence (ROI). The ROI is a critical design parameter for a field system because an overestimated ROI will lead to inadequate subsurface treatment, while an underestimated ROI will lead to an unnecessary number of wells (Semer and Robin, 1998).

3. Objectives and Scope

The goal of this research is to understand the effect of EM waves on air sparging. This work mainly consists of the main objective of performing an experimental study of the effect of EM waves (specifically the electric-field component) on parameters and characteristics controlling air sparging effectiveness. These characteristics and parameters are air diffusion rate, especially between air channels in saturated soils and the formation (i.e., shape and size) of air channels during air sparging. Another main objective is to evaluate how EM waves' frequency can be controlled to reduce the heat in order to maintain the temperature of the medium while simultaneously stimulating the airflow.

To study the effects of EM stimulation on airflow in saturated soils, the air is injected at three pressure levels into a saturated glass-bead medium contained within a resonant cavity structure. The glass beads are Ballotini impact beads with the specific gravity of 2.46 g/cm³.

The resonant cavity was used in order to provide a controlled electric-field pattern within the medium under study. A loop antenna was used as the source of EM waves to stimulate the medium within the cavity. A vertically polarized monopole probe was used to measure the electric field within the cavity. The vertical component of the electric field dominates this measurement due to the vertical polarization of the probe. The electric field was also simulated in COMSOL Multiphysics and validated against the experimental measurements to provide a validated numerical model to achieve the 3D vector electric field.

4. Laboratory Experimentation

The experiments of this work were performed in a 61.5-cm × 40-cm × 15-cm clear acrylic tank with 0.5-cm thick walls. All walls and top surface of the box are covered with grounded, transparent, electrically conductive films. The bottom is covered with aluminum tapes sharing the same ground. The digital imaging from one side of the tank was performed to quantitatively analyze the airflow induced into the fully water-saturated glass-bead medium using a Cannon Rebel T2i 18-Megapixel digital camera.

Figure 1a shows the test apparatus and the injection well used for the EM simulation of air sparging. Three perforated Acrylic panels covered with geotextile fabric were placed at the bottom and the two sides of the tank. An inflow valve was placed at the front of the tank at a height of 3 cm above the tank bottom. Two outflow valves were placed at both sides of the tank at the height of 20 cm above the tank bottom.

CPVC tubes were used to simulate the air-injection well. The tube featured a 2.15-cm outside diameter and a 1.6-cm inside diameter. The tubes have several holes with the diameter of 1.5mm along the lower 3.8 cm of the tube to allow for air injection. An acrylic plate is placed above the tank to support the tube in its proper location within the box. The tube, used for air injection, is placed in the middle of the top plate with its plugged bottom resting 3 cm above the tank bottom. The injection tube is connected to an air-supply faucet in the Clean Soil lab (Room 3104) in the Environmental Research Building (ERB) at Boise State University.

The opacity of natural soils prevents the direct observation of airflow patterns during air sparging. Hence, transparent glass beads were used in this test to simulate the natural soil and facilitate visual observation. Deionized, deaerated water was used in all experiments.

Wet pluviation was used for glass-bead medium preparation. Wet pluviation method is a specimen preparation technique, very well suited for preparation of large fully homogeneous, water-saturated specimens. In this method, water is first placed into the acrylic box up to a predetermined level. As mentioned, glass beads were then gently poured into the water

using the wet pluviation technique through a funnel located 20 cm above the water table, (Vaid and Negussey, 1998). The glass beads were then be gently smoothed over. This process is performed carefully to avoid the creation of layering to avoid creation of preferential air passage paths. This procedure was continued until the desired thickness of the medium was reached.

At this step of the test, air was injected into the saturated glass-bead medium with and without EM stimulation at various EM frequencies and power levels to evaluate the effect of EM stimulation on already formed channels or initiation of air-channel formation (i.e., size, and shape) under different air-pressure levels.

A signal generator is used as the source of EM waves. The signal generator is connected to an amplifier to amplify the power launched into the medium to enable examining various power intensities at each frequency of operation. Other devices are a Vector Network analyzer, a Spectrum Analyzer, a matching network, and a dual-directional coupler (Figure 1b). The antenna used to excite the medium is a loop antenna made out of an RG-8 coaxial cable. The loop antenna was placed near one side of the tank and submerged in the saturated medium.

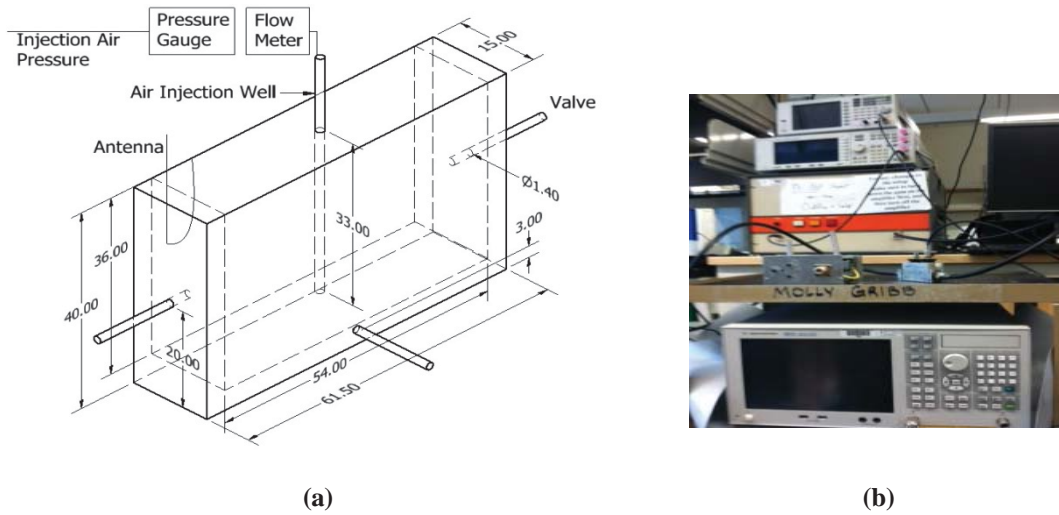


FIG. 1. (a) Schematic diagram of experiment box (b) Setup and devices used for EM stimulation tests (All measurements are in cm).

As mentioned, air was injected at different pressure levels with and without EM stimulation. Then, the effect of EM stimulation on the airflow pattern was monitored using digital imaging. The grain-size distribution of the glass beads is shown in Figure 2.

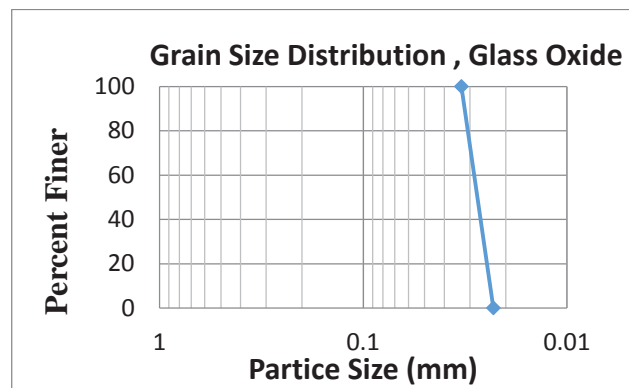


FIG. 2. Grain-size distribution of glass beads

4.1. Test Procedure

As mentioned, to study the effect of EM waves on airflow, two series of experiments were conducted in this study.

- I. The first series of tests were performed in order to study the air flow pattern without application of EM waves in three glass-bead medium condition: (i) a stratified soil profile with a 4-cm thick partially saturated layer above the fully saturated soil (referred to as Medium 1); (ii) a stratified soil profile with a 12-cm thick partially saturated layer above the fully saturated layer (referred to as Medium 2); and (iii) a homogenous fully saturated soil (referred to as Medium 3).
- II. The second series of experiments studied the EM effect on air channels. However, this, itself, is divided into two categories: (Category 1) the EM effect on air-channel initiation and (Category 2) the EM effect on already formed channels. The tests are again conducted at the following three medium conditions: (i) the stratified soil profile with a 4-cm thick partially saturated layer on top of the saturated soils (Medium 1); (ii) the stratified soil profile with a 12-cm thick partially saturated layer on top of the saturated soils (Medium 2); (iii) the 36-cm homogenous fully-saturated medium. All of these cases were objected to air injection without the application of a vacuum (Table 1). Table 1 shows a summary of these medium conditions.

Table 1. Properties of glass-bead samples

Sample No.	Particle Size (mm)	U.S. Sieve #	Height of Saturated Layer (cm)	Height of Unsaturated Layer (cm)	Porosity
Sample 1	0.6-0.85	20-30	24	4	0.6
Sample 2	0.6-0.85	20-30	24	12	0.6
Sample 3	0.6-0.85	20-30	36	0	0.6

The electric field was mapped in the region under test using a 50- Ω , RG-402, coaxial probe to create a 3D map of the electric field. The electric-field pattern was also simulated using the COMSOL software, which was validated against the experimentally mapped electric field.

The location of the air-injection well remained constant for all tests. The air-injection pressure was varied from 20 kPa to 100 kPa at 10-kPa increments. The EM power was varied from 10 to 30 W at 10-W increments, at appropriate frequencies governed by the success at matching the impedance of the setup to the 50- Ω impedance of the amplifier. At this stage of the work, the water within the box was at a no-flow steady-state for all tests.

5. Observed Airflow Patterns

5.1. Unstimulated Tests

The first series of experiments featured 0.08-mm glass-bead as a simulant for the soil medium; without applying the EM waves. Both saturated and unsaturated zones were prepared using wet and dry pluviation, and subjected to no-flow static water level. Air injection into the medium started at 20 kPa pressure with constant airflow rate during all these tests. The airflow pattern was observed using the camera located across from the front face of the box.

- I. When air was injected into Sample 1, it moved in channels, and the ZOI was cone shaped. The pressure was then increased at 10-kPa increments, and the flow pattern was again observed. When the air-injection pressure was increased to 100 kPa, the size of the ZOI did not change, but the concentration of air channels did increase. The maximum radius of influence (ROI) was measured to be 16 cm. The radius of influence (ROI) remained at 16 cm when the air-injection pressure was increased to 120 KPa. Based on these results, a limit in the size of the radius of influence (ROI) has been reached. In other words, more pressure might increase the concentration of air within channels, but the size of the ROI will not change.
- II. This second series of tests featured the same conditions, except the thickness of partially saturated zone was 12 m (Sample 2). Air-injection again started at 20 kPa. The results shows that air moved in channels, but the ROOI increased in comparison with the ROI in Sample 1. The results of this test also illustrate that the size of

ROI will not increase in spite of the increase the the air-injection pressure; although the concentration of air within air channels increased. The results show the size of ROI increased by the increase in the initial air-injection pressure. The radius of influence increased to 21.5 cm when an injection pressure of 80 kPa was used. The ROI remained constant (21.5 cm) when the pressure was increased further up to 120 kPa. Based on these results, a limit in the size of the ROI has been reached in smaller air-injection pressures in comparison with the previous results. The results of these two tests are shown in Figure 3.

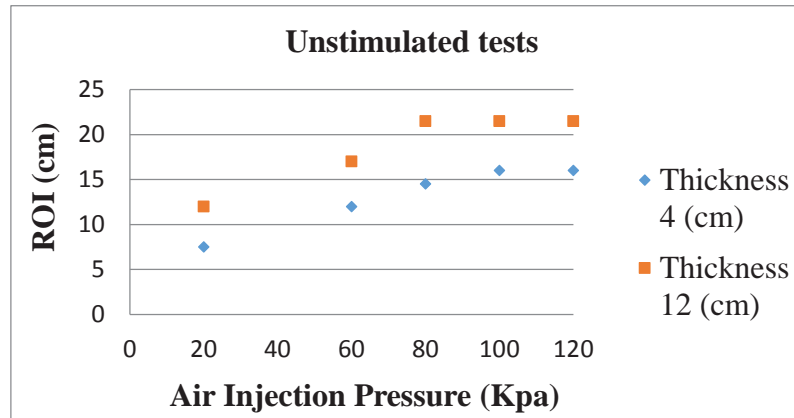


FIG. 3. The Size of radius of influence (ROI) for Sample 1 and Sample 2

- III. This third series of tests was conducted within the fully saturated medium (Sample 3), and the medium was observed from above. The airflow rate and injection pressures were constant like the previous tests. The size of the ROI increased by the increase in the initial air-injection pressure.

In all unstimulated tests, the ZOI was asymmetric with the injection pipe as the axis of symmetry. Another noteworthy observation is that fully formed channels are very stable and hard to change. Therefore, within the unstimulated test, no increase in air-injection pressure changes the ZOI shape and ROI size of already formed channels.

5.2. Stimulated Tests

5.2.1. Effect of EM Waves on Already-Formed Air Channels

The next series of tests were performed with the same samples, constant airflow rate, and same range of air-injection pressure, except EM energy is applied to the system. The medium was stimulated at different frequencies controlled based on the quality of the impedance matching achieved and monitored through maintaining the reflected power into the amplifier below its 1-W reflected power tolerance, monitored using the spectrum analyzer. Stimulated tests were performed at 65, 67.5, 115, and 191.7 MHz. They were also performed at different RF power of 10, 20, and 30 W (and 50 Watts only for the frequency of 115 MHz) to investigate the power level effect. Air was injected into the glass-bead medium 15 minutes after air channels are formed. The results were observed for 30 minutes of EM stimulation. The size of the ROI and shape of the ZOI for Sample 1, Sample 2, and Sample 3 were observed to be similar to the unstimulated tests. Even with the increase in the applied power, the size and shape of the ZOI of air channels that are already formed did not change.

In other words, formed channels are very stable and hard to change. Therefore, similar to the unstimulated test where no increase in pressure changed the already formed channels, no EM power can change the ZOI shape and ROI size of already formed channels.

5.2.2. Effect of EM Waves on Initiation of Air-Channel Formation

In these tests, the medium was first stimulated at each of the above-mentioned frequencies and power levels of 10, 20, and 30 W for each frequency for all samples. After 30 minutes of EM stimulation, the air-injection was initiated. The air flow pattern was observed against the front face of the tank, about 15 minutes after air channels are formed within

Samples 1 and 2. The size of ROI and the shape of ZOI did not change even at higher magnitudes of power. However, when the air was injected into the saturated medium (Sample 3) when the medium was being stimulated at different frequencies, and the results were observed from above the box. Only when the medium was stimulated at the frequency of 191.7 MHz at power 10 W or higher, the results show a change in the size of ROI and the shape of the ZOI in comparison with the unstimulated case.

This could be due to the fact that 191.7 MHz is the first resonance mode for a cavity of this size, where the electric field is maximum at the air-injection point. In other words, to study the sheer effect of frequency independent of the cavity size, several cavities should be tested at their corresponding resonant frequencies where electric field is maximum at the air-injection point for all those cases.

Due to the saturated condition and the absence of a partially saturated zone, the locations of exiting air would be readily, because of local agitation. The ZOI became significantly irregular when the medium was stimulated at the frequency of 191.7 MHz and the ZOI shifted 2 cm to. The reason and mechanism behind this shift needs to be studied further in the future. One potential mechanism is dielectrophoresis. Although change in the ZOI and ROI was successfully observed at 191.7 MHz EM simulation, all these test were performed for other frequency as well.

To investigate the effect of the power level, the test for Sample 3 at frequency 191.7 MHz was then repeated at 20 and 30 W. The ZOI becomes more and more irregular and shifts more to right hand side of the box. Unlike the test at 191.7 MHz, during the stimulation at other frequencies, the airflow pattern was observed to be axisymmetric with the air-injection pipe as the axis of symmetry (similar to the unstimulated tests). Figure 4 shows experimentally measured and simulated contour maps of electric field on a typical depth (vertical) slice at 191.7 MHz. This slice is 0.1 cm from the center of the box

As mentioned, the electric field was both simulated and experimentally measured. The simulated results will be later used to study the pattern of the electric field and its gradient to understand the potential mechanism behind the EM effect on the initiation of air-channel formation. Dielectrophoresis is a potential candidate mechanism behind this effect where the electric-field radiation pattern is needed for through understanding and analysis.

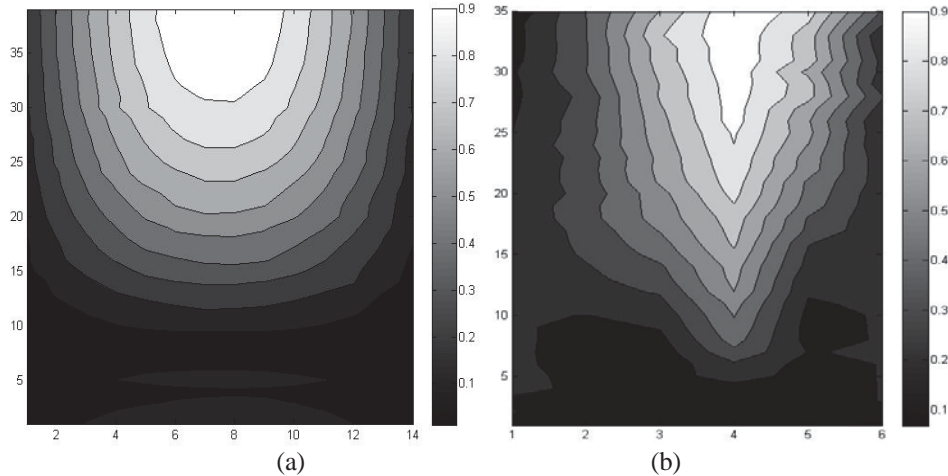


FIG. 4. Normalized electric-field contour-map: (a) simulation; and (b) experimental measurements. The contourmaps are plotted on a depth (vertical) slice located 2 cm from the center of the box toward the antenna.

5.2.3. Temperature Effects

The temperature of the medium close to the antenna body was recorded at frequency 191.7 MHz in order to differentiate the effect of temperature on the air flow channels from the effect of RF waves. As expected, the temperature slightly increased for this frequency. The maximum change in temperature was less than 1°C within the period of the experiment. Figure 5 indicate the rise in the temperature at 191.7 MHz.

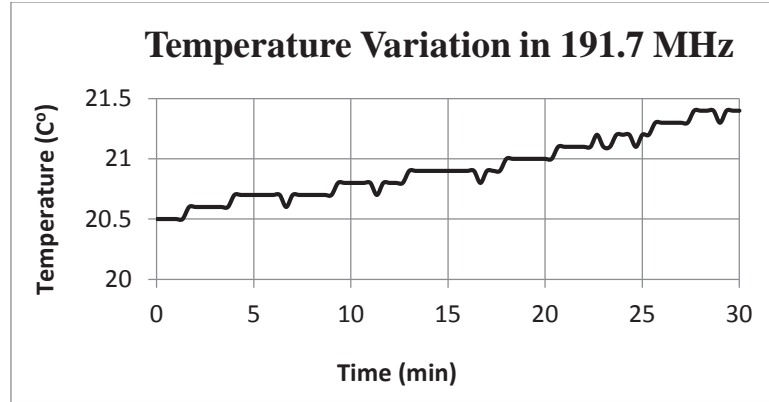


FIG. 5. Temperature of glass-bead medium monitored 1.5 cm horizontally away from the loop antenna in the X direction at frequency 191.7 MHz over 30 minutes for and RF power of 30 W.

Conclusion

When the air is injected into the saturated zone, the observed air channels, the size of radius of influence (ROI), and the size of the zone of influence (ZOI) will depend on the initial air-injection pressure.

Already formed air channels are very stable. Hence, increasing the air-injection pressure after the formation of air channels at any initial air pressure will not change the size and shape of air channels. However, the concentration of air within channels is the only factor that will increase with the increase in the pressure. Once air channels are formed within glass-bead medium at any initial air-injection pressure, any increase or decrease in the air-injection pressure cannot affect the size of the zone of influence. The increase in the initial air-injection pressure, however, increases the size of radius of influence.

The thickness of the partially saturated zone above the saturated zone affects the size of the ROI. The ROI observed in the three samples with thicker partially saturated zones are greater than those of thinner partially saturated zones. Samples with thicker partially saturated zone require lower pressure to reach the maximum possible radius of influence than that required for the samples with thinner partially saturated zones.

Similarly, applying EM waves after formation of air channels will not effect the size and shape of air channels. This is, again, simply because already formed air channels are very stable.

Initiation of air channel formation will however be affected by EM stimulation. The shape of ZOI will be more irregular and will shift at the frequency 191.7 MHz at power levels above 10 W. Increasing the power level at this frequency will render the shape of the ZOI mire irregular and cause larger shifts

Acknowledgement

This project was supported by the National Science Foundation through the Interdisciplinary Research (IDR) program, CBET Award No. 0928703.

References

- Elder, Carl R. and Benson, Craig H. (1999). "Air Channel Formation, Size, Spacing, and Tortuosity during air Sparging." *National Ground Water Association (GWMA)*: 171-181.
- Braida, W. and Ong, S.K. (2001). "Air sparging Effectiveness: Laboratory characterization of air channel mass transfer zone for VOC volatilization." *Journal of Hazardous Materials*. B87: 241-258.
- Benner, M.L., Mihtar, R.H., and Lee, L.S. (2002). "Factors affecting air sparging remediation system using field data and numerical simulations." *Journal of Hazardous Materials*. B95: 304-329.
- Suthersan, S.S., and Raton Sangrey, B. (1999). "IN SITU Air SPARGING, Remediation engineering, design concepts", CRC Press LLC < Online at <http://www2.bren.ucsb.edu/~keller/courses/esm223/SuthersanCh04AirSparge.pdf>>
- Balanis, C.A. (1989). *Advanced Engineering Electromagnetics*, John Wiley and Sons Inc., ISBN 0-471-62194-3
- Semer, Robin (Robin A.), *Air sparging: contaminant removal mechanisms parameterization comparisons, and enhancement*. Master thesis, 1998
- Bayat, E.E., Yegian, M K., Alshwabkeh, A., and Geokyer, S. (Jun 2009). "A NEW mitigation technique for preventing liquefaction-induced building Damages during earthquakes." *WCCE – ECCE – TCCE Joint Conference: EARTHQUAKE & TSUNAMI*.
- Vaid, Y.P., and Negussey, D. (1998). "Preparation of reconstituted sand specimens." *Advanced triaxial testing of soil and rock, ASTM STP 977*, Philadelphia: 405-417.